

Balance and frustration in signed networks

SAMIN AREF[†]

Department of Computer Science, University of Auckland, Private Bag 92019, Auckland, New Zealand

[†]Corresponding author. Email: sare618@aucklanduni.ac.nz

AND

MARK C. WILSON

Department of Computer Science, University of Auckland, Private Bag 92019, Auckland, New Zealand

Edited by: Ernesto Estrada

[Received on 20 April 2018; editorial decision on 2 July 2018; accepted on 6 July 2018]

The frustration index is a key measure for analysing signed networks, which has been underused due to its computational complexity. We use an exact optimization-based method to analyse frustration as a global structural property of signed networks coming from diverse application areas. In the classic friend-enemy interpretation of balance theory, a by-product of computing the frustration index is the partitioning of nodes into two internally solidary but mutually hostile groups. The main purpose of this article is to present general methodology for answering questions related to partial balance in signed networks, and apply it to a range of representative examples that are now analysable because of advances in computational methods. We provide exact numerical results on social and biological signed networks, networks of formal alliances and antagonisms between countries, and financial portfolio networks. Molecular graphs of carbon and Ising models are also considered. The purpose served by exploring several problems in this article is to propose a single general methodology for studying signed networks and to demonstrate its relevance to applications. We point out several mistakes in the signed networks literature caused by inaccurate computation, implementation errors or inappropriate measures.

Keywords: frustration index; line index of balance; signed graph; integer programming; optimization; balance theory.

Mathematics Subject Classification (MSC 2010): 05C22, 90C35, 90C90, 90C09, 90C10

1. Introduction

The theory of structural balance introduced by Heider [1] is an essential tool in the context of social relations for understanding the impact of local interactions on the global structure of signed networks. Following Heider, Cartwright and Harary identified cycles containing an odd number of negative edges [2] as a source of tension that may influence the structure of signed networks in particular ways. Signed networks in which no such cycles are present satisfy the property of structural balance, which is considered as a state with minimum tension [2].

For graphs that are not balanced, a distance from balance (a measure of partial balance) can be computed [3]. In the past few decades, different measures of balance have been suggested. Measures based on cycles [2, 4–7], triangles [8, 9] and eigenvalues of the adjacency matrix [9–12] are not generally consistent [3] and result in conflicting observations [12–14]. A recent study [3] compares all these

measures and concludes that substantially different levels of partial balance are observed under cycle-based [2, 4–9], eigenvalue-based [9–12] and frustration-based [5, 14–16] measures of balance.

Among various measures is the *frustration index* that indicates the minimum number of edges whose removal (or equivalently, negation) results in balance [5, 15, 16]. The clear definition of the frustration index allows for an intuitive interpretation of its values as the minimum number of edges that keep the network away from a state of total balance (an edge-based distance from balance). In this study, we focus on applications of the frustration index, also known as *the line index of balance* [5], in different contexts beyond the structural balance of signed social networks.

Satisfying essential axiomatic properties as a measure of partial balance [3], the frustration index is a key to frequently stated problems in many different fields of research [17–20]. In biological networks, optimal decomposition of a network into monotone subsystems is made possible by calculating the frustration index of the underlying signed graph [17]. In physics, the frustration index provides the ground state of atomic magnet models [18, 21]. In international relations, the dynamics of alliances and enmities between countries can be investigated using the frustration index [19]. Frustration index can also be used as an indicator of network bi-polarization in practical examples involving financial portfolios. For instance, some low-risk portfolios are shown to have an underlying balanced signed graph containing negative edges [22]. In chemistry, bipartite edge frustration can be used as a stability indicator of carbon allotropes known as fullerenes [20, 23].

2. Computing the frustration index

From a computational viewpoint, computing the frustration index of a signed graph is an NP-hard problem equivalent to the ground state calculation of an Ising model without special structure [24–26]. Computation of the frustration index also reduces from classic unsigned graph optimization problems (EDGE-BIPARTITION and MAXCUT), which are known to be NP-hard [27].

The frustration index can be computed in polynomial time for planar graphs [27, 28]. In general graphs, however, the frustration index is even NP-hard to approximate within any constant factor [27]. There has been a lack of systematic investigations for computing the exact frustration index of large-scale networks [29, 30]. In small graphs with fewer than 40 nodes, exact computational methods [31–34] are used to obtain the frustration index. More recent studies focus on approximating [35–38] and computing [29, 30] the frustration index in large signed graphs with at least thousands of edges.

A closely related and more general problem (that is beyond our discussions in this article) is finding the minimum number of edges whose removal results in a weakly balanced signed graph (as in Davis's definition of *weak balance* [39]). This problem is referred to as the *Correlation Clustering* problem [40, 41], which is investigated more comprehensively in the literature [34, 40, 42–45]. A comparison of mathematical programming models for computing the frustration index and correlation clustering can be found in [29, subsection 8.2].

Faccchetti *et al.* [14] suggested a non-linear energy function minimization model for finding the frustration index. Their model was used as the basis of various non-exact optimization techniques [17, 41, 46–48]. Using heuristic algorithms [17], estimations of the frustration index have been provided for biological networks up to 1.5×10^3 nodes [17] and social networks with up to 10^5 nodes [14, 49]. Doreian and Mrvar [19] have provided some upper bounds on the frustration index of signed international relation networks [50]. We use their dataset in Section 7 and analyse it using the exact values of the frustration index.

In this study, we use a recently developed optimization model [29] that computes the frustration index of large-scale signed networks exactly and efficiently.

Our contribution

We focus on the frustration index of signed networks, a standard measure of balance mostly estimated or approximated for decades due to the inherent combinatorial complexity. We continue a line of research begun in [3] (which compared various measures of partial balance and suggested that the frustration index should be more widely used), [30] (which explained how integer linear optimization models can be used to compute the frustration index) and [29] (which substantially improves the efficiency of such computations using algorithmic refinements and powerful mathematical programming solvers).

The purpose of the present article is to present a single general methodology for studying signed networks and to demonstrate its relevance to applications. We consider a variety of signed networks arising from several disciplines. These networks differ substantially in size and the computational results require different interpretations. The current implementation of our algorithms can efficiently provide exact results on networks with up to 100 000 edges. A by-product of exactly computing the frustration index is an optimal partitioning of nodes into two groups where the number of intra-group negative edges and inter-group positive edges is minimized.

This article begins by laying out the theoretical dimensions of the research in Section 3. The computational method is briefly discussed in Section 4 followed by a discussion on its efficiency. Numerical results on signed networks of six disciplines are provided in Sections 5–9. Section 10 provides a short conclusion and suggests future directions. Along the way, we point out several mistakes in the signed networks literature caused by inappropriate measures and inaccurate computation.

3. Preliminaries

We recall some standard definitions.

3.1 Notation

We consider undirected signed networks $G = (V, E, \sigma)$. The ordered set of nodes is denoted by $V = \{1, 2, \dots, n\}$, with $|V| = n$. The set E of edges can be partitioned into the set of positive edges E^+ and the set of negative edges E^- with $|E| = m$, $|E^-| = m^-$ and $|E^+| = m^+$ where $m = m^- + m^+$. The sign function is denoted by $\sigma : E \rightarrow \{-1, +1\}$.

We represent the m undirected edges in G as ordered pairs of vertices $E = \{e_1, e_2, \dots, e_m\} \subseteq \{(i, j) \mid i, j \in V, i < j\}$, where a single edge between nodes i and j , $i < j$, is denoted by (i, j) , $i < j$. We denote the graph density by $\rho = 2m/(n(n - 1))$.

The entries of the symmetric adjacency matrix \mathbf{A} are defined in Eq. (1).

$$a_{ij} = \begin{cases} \sigma_{(i,j)} & \text{if } (i,j) \in E \\ \sigma_{(j,i)} & \text{if } (j,i) \in E \\ 0 & \text{otherwise} \end{cases} \quad (1)$$

We use $G_r = (V, E, \sigma_r)$ to denote a reshuffled graph in which the sign function σ_r is a random mapping of E to $\{-1, +1\}$ that preserves the number of negative edges.

A *walk* of length k in G is a sequence of nodes $v_0, v_1, \dots, v_{k-1}, v_k$ such that for each $i = 1, 2, \dots, k$ there is an edge from v_{i-1} to v_i . If $v_0 = v_k$, the sequence is a *closed walk* of length k . If the nodes in a closed walk are distinct except for the endpoints, the walk is a cycle of length k . The *sign* of a walk or cycle is the product of the signs of its edges. Cycles with positive (negative) signs are balanced (unbalanced). A balanced graph is one with no unbalanced cycles.

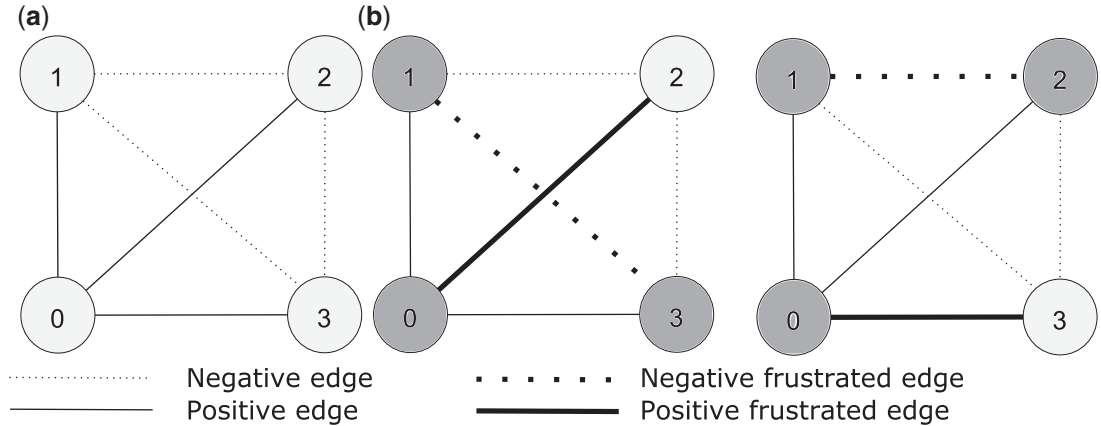


FIG. 1. The impact of node colouring on the frustration of edges. (a) An example signed graph. (b) Two different node colourings (both optimal) and their resulting frustrated edges.

3.2 Frustration count

For any signed graph $G = (V, E, \sigma)$, we can partition V into two sets, denoted $X \subseteq V$ and $\bar{X} = V \setminus X$. We call X a colouring set and we think of this partitioning as specifying a colouring of the nodes, where each node $i \in X$ is coloured black, and each node $i \in \bar{X}$ is coloured white. We let x_i denote the colour of node $i \in V$ under X , where $x_i = 1$ if $i \in X$ and $x_i = 0$ otherwise. Considering node colours is a standard way of defining discrete decision variables for nodes in modelling graph optimization problems.

Figure 1(a) demonstrates an example signed graph in which positive and negative edges are represented by solid lines and dotted lines respectively. Figure 1(b) illustrates two node colourings and the resulting frustrated edges represented by thick lines.

We define the *frustration count* $f_G(X)$ as the number of frustrated edges of G under X :

$$f_G(X) = \sum_{(i,j) \in E} f_{ij}(X)$$

where $f_{ij}(X)$ is the frustration state of edge (i,j) , given by

$$f_{ij}(X) = \begin{cases} 0, & \text{if } x_i = x_j \text{ and } (i,j) \in E^+ \\ 1, & \text{if } x_i = x_j \text{ and } (i,j) \in E^- \\ 0, & \text{if } x_i \neq x_j \text{ and } (i,j) \in E^- \\ 1, & \text{if } x_i \neq x_j \text{ and } (i,j) \in E^+ \end{cases} \quad (2)$$

The frustration index $L(G)$ of a graph G can be obtained by finding a subset $X^* \subseteq V$ of G that minimizes the frustration count $f_G(X)$, i.e. solving Eq. (3).

$$L(G) = \min_{X \subseteq V} f_G(X) \quad (3)$$

4. Methods and materials

In this section, we discuss a mathematical programming model in Eq. (4) that minimizes the frustration count as the objective function over binary decision variables defined for nodes and edges of the graph. Note that, there are various ways to formulate the frustration count using variables defined over graph nodes and edges leading to various mathematical programming models that are investigated in detail in [29].

4.1 Methodology

Computing the frustration index can be formulated as a binary linear model that counts the frustrated edges using binary variable $f_{ij} \forall (i,j) \in E$ to denote frustration of edge (i,j) and $x_i \forall i \in V$ to denote the colour of node i . Constraints of the optimization model are formulated according to the values of f_{ij} in Eq. (2). Therefore, the minimum frustration count under all node colourings is obtained by solving (4):

$$\begin{aligned} \min_{x_i, f_{ij}} Z = & \sum_{(i,j) \in E} f_{ij} \\ \text{s.t. } & f_{ij} \geq x_i - x_j \quad \forall (i,j) \in E^+ \\ & f_{ij} \geq x_j - x_i \quad \forall (i,j) \in E^+ \\ & f_{ij} \geq x_i + x_j - 1 \quad \forall (i,j) \in E^- \\ & f_{ij} \geq 1 - x_i - x_j \quad \forall (i,j) \in E^- \\ & x_i \in \{0, 1\} \quad \forall i \in V \\ & f_{ij} \in \{0, 1\} \quad \forall (i,j) \in E \end{aligned} \tag{4}$$

Several techniques are used to speed up the branch and bound algorithm for solving the binary programming model in Eq. (4) and the like as discussed in [29, 30]. We implement the three speed-up techniques known as pre-processing data reduction, prioritized branching and fixing a colour, and unbalanced triangle valid inequalities [29, 30] and solve the optimization problem using Gurobi Optimization Inc. [51]. Details of the optimization model and speed-up techniques can be found in [29, 30].

Aref *et al.* have tested their optimization models [29, 30] on synthetic and real-world datasets using ordinary desktop computers showing the efficiency of their models in computing the frustration index in comparison to other models in the literature [17, 19, 27, 31–35, 52, 53]. For detailed discussions on the efficiency of the binary linear programming model in Eq. (4), one may refer to [29].

For comparing the level of frustration among networks of different size and order, we use the *normalized frustration index*, $F(G) = 1 - 2L(G)/m$. This standard measure of partial balance is suggested in a comparative study of structural balance measures because it satisfies key axiomatic properties [3]. Values of $F(G)$ are within the range of $[0, 1]$ and greater values of $F(G)$ represent closeness to a state of structural balance.

Our baseline for evaluating balance comprises the average and standard deviation of the frustration index in reshuffled graphs (that have signs allocated randomly to the same underlying structure). Accordingly, we use Z score values, $Z = (L(G) - L(G_r))/SD$, in order to evaluate the level of partial balance precisely.

4.2 Materials

We use a wide range of examples from different disciplines all being undirected signed networks. This includes four social signed networks ranging in size from 49 to 99 917 edges in Section 5, four biological signed networks with 779–3215 edges in Section 6, one dynamic network of international relations with 51 time windows ranging in size from 362 to 1247 edges in Section 7, six financial portfolios with 10–55 edges over 9 years in Section 8 and molecular fullerene graphs with 270–9000 edges and Ising models with 32–79 600 edges in Section 9. The datasets used in this study are made publicly available on the Figshare research data repository [54]. We use a wide variety of datasets, rather than focusing on a specific application, in order to underline the generality of our approach.

The fundamental reason why we only use undirected signed networks is that the reliability test for predictions on directed signed networks made by balance theory shows very negative results [13]. Based on large directed signed networks such as Epinions, Slashdot and Wikipedia, the binary predictions made by balance theory are incorrect almost half of the time [13]. This observation supports the inefficacy of balance theory for structural analysis of *directed* signed graphs [3].

The numerical results in this article are obtained by solving the binary linear programming model (4) coupled with three speed-up techniques [29] using Gurobi's Python interface [51]. Unless stated otherwise, the hardware used for the computational analysis is a virtual machine with 32 Intel Xeon CPU E5-2698 v3 @ 2.30 GHz processors and 32 GB of RAM running 64-bit Microsoft Windows Server 2012 R2 Standard.

5. Social networks

In this section, we discuss using the frustration index to analyse social signed networks inferred from the sociology and political science datasets.

5.1 Datasets

We use well-studied datasets of communities with positive and negative interactions and preferences. This includes Read's dataset for New Guinean highland tribes [55] and the last time frame of Sampson's data on monastery interactions [56]. Our analysis also includes a signed network of US senators that is inferred in [57] through implementing a stochastic degree sequence model on Fowler's Senate bill co-sponsorship data [58] for the 108th US senate.

A larger social signed network we use is from the Wikipedia election dataset [13]. This dataset is based on all adminship elections before January 2008 in which Wikipedia users have voted for approval or disapproval of other users promotions to becoming administrators. We use an undirected version of the Wikipedia elections signed graph made publicly available in [44]. The four social signed networks are illustrated in Figure 2 where green and red edges represent positive and negative edges, respectively.

5.2 Results

Our numerical results are shown in Table 1 where the average and standard deviation of the frustration index in 500 reshuffled graphs (50 reshuffled graphs for Wikipedia election network), denoted by $L(G_r)$ and SD, are also provided for comparison.

As it is expected the four social signed networks are not totally balanced. However, the relatively small values of $L(G)$ suggest low levels of frustration in these networks. In order to be more precise, we have implemented a very basic statistical analysis using Z scores $Z = (L(G) - L(G_r))/SD$. These Z

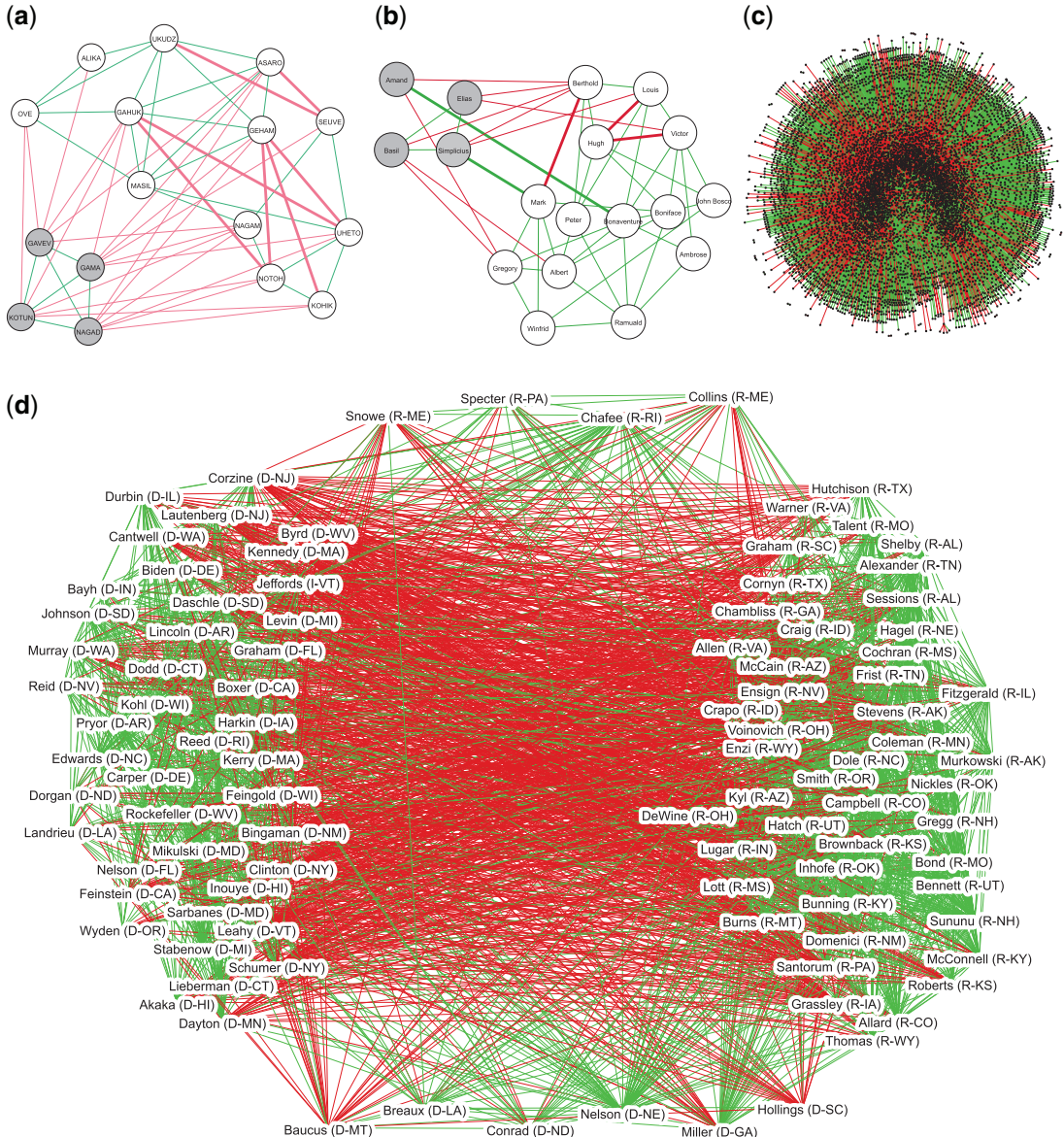


FIG. 2. Four signed networks inferred from the sociology and political science datasets and visualized using Gephi. (a) Optimal colouring of New Guinean tribes network with frustrated edges shown by thick lines [55]. (b) Optimal colouring of monastery interactions network with frustrated edges shown by thick lines [56]. (c) Network of Wikipedia elections [13]. (d) Network of the 108th US senate (nodes having mismatching party colour and optimal colour are positioned on the top and bottom.) [57].

TABLE 1 *The frustration index in social signed networks*

Graph (n, m, m^-)	ρ	$L(G)$	$L(G_r) \pm SD$	Z score
Highland tribes (16, 58, 29)	0.483	7	14.65 ± 1.38	-5.54
Monastery interactions (18, 49, 12)	0.320	5	9.71 ± 1.17	-4.03
US senate (100, 2461, 1047)	0.497	331	965.6 ± 9.08	-69.89
Wiki elections (7112, 99 917, 21 837)	0.004	14532	$18936.1 \pm 45.1^\dagger$	-97.59 [†]

[†] Based on lower bounds within 15% of the optimal solution.

scores, provided in the right column of the Table 1, show how close the networks are to a state of balance. The results indicate that networks exhibit a level of frustration substantially lower than what is expected by chance.

The levels of balance in the three networks of Highland tribes, Monastery interactions and US senate were previously measured in [3] using not only the frustration index, but also measures based on triangles and eigenvalues [8–10]. For these three networks, which have comparatively high densities, the levels of balance measured using triangles and eigenvalues were reported to be consistent with the results that the frustration index provides [3].

5.3 Partitions

In the network of US senators, we may get insight not only from the value of the frustration index, but also the optimal node colouring leading to the minimum number of frustrated edges. As shown in node labels of Figure 2d, the 108th US senate was made of 48 Democratic senators, 1 independent senator (caucusing with Democrats) and 51 Republican senators. Based on these figures, we may consider a party colour for each node i in the network and position senators from different parties on the left (Democrat) and right (Republican) sides of Figure 2d. The abundance of green edges on the left and right sides of Figure 2d shows that most senators have positive relationship with their party senators (co-sponsor bills proposed by their party). The numerous red edges between left and right sides of Figure 2d show opposition between senators from different parties (senators do not support bills put forward by the other party in most cases).

We can also compare the party colour for each node i to the optimal colour (x_i optimal value) that leads to the partitioning with the minimum number of frustrated edges. As expected from the bi-polar structure of US senate, the colours match in 90 out of 100 cases (considering the independent senator as a Democrat). The nodes associated with Republican (Democrat) senators who have mismatching party colour and optimal node colour are positioned on the top (bottom) of Figure 2d. It can be observed from such nodes that, contrary to the other nodes, they have negative (positive) ties to their (the other) party.

5.4 Computations

Regarding performance of the optimization model, a basic optimization formulation of the problem with no speed-up technique (such as [30, Eq. 8]) would solve the Highland tribes and Monastery interaction instances in a reasonable time on an ordinary computer [30]. The binary linear programming model (4) solves such instances in split seconds, while for the senators network it takes a few seconds.

For Wikipedia elections network, 9.3 hours of computation is required to find the optimal solution. This considerable computation time prevents us from testing 500 reshuffled versions of the Wikipedia elections network. In order to perform the statistical analysis for the Wikipedia network in a reasonable time, we limited the number of runs to 50.

As a conservative approach, we also used the average of best lower bound obtained within 15% of the optimal solution as $L(G_r)$ for Wikipedia elections network. This approach reduces the average computation time of each run to 4 hours. The branch and bound algorithm guarantees that the frustration index of each reshuffled graph (which remains unknown) is greater than the lower bound we use to compute the Z score for Wikipedia elections network.

6. Biological networks

Some biological models are often used to describe interactions with dual nature between biological molecules in the field of systems biology. The interactions can be *activation* or *inhibition* and the biological molecules are enzymes, proteins or genes [35]. This explains the parallel between signed graphs and these types of biological networks. Interestingly, the concept of *close-to-monotone* [59] in systems biology is analogous to being close to a state of balance. Similar to negative cycles and how they lead to unbalance, existence of *negative loops* in biological networks indicates a system that does not display well-ordered behaviour [59].

6.1 Datasets

There are large-scale gene regulatory networks where nodes represent genes and positive and negative edges represent *activating connections* and *inhibiting connections*, respectively. We use four signed biological networks previously analysed by [17]. They include two gene regulatory networks, related to two organisms: a eukaryote (the yeast *Saccharomyces cerevisiae*) [60] and a bacterium (*Escherichia coli*) [61]. Another signed network, we use is based on the epidermal growth factor receptor (EGFR) pathway [62]. EGFR is related to the epidermal growth factor protein whose release leads to rapid cell division in the tissues where it is stored such as skin [35]. We also use a network based on the molecular interaction map of a white blood cell (macrophage) [63].

Yeast and *E. coli* networks are categorized as transcriptional networks while EGFR and macrophage are signalling networks [17]. Figure 3 shows three of these biological signed networks. The colour of edges correspond to the signs on the edges (green for activation and red for inhibition). For more details on the four biological datasets, one may refer to [17].

6.2 Results

Table 2 provides the results for the four biological networks where the average and standard deviation of the frustration index in 500 reshuffled graphs are also provided for comparison.

The results in Table 2 show that the level of frustration is very low for yeast and *E. coli* networks. The Z score value for the yeast network is -16.75 , which is consistent with the observation of DasGupta *et al.* (based on approximating the frustration index) that the number of edge deletions is up to 15 standard deviations away from the average for comparable random and reshuffled graphs [35, Section 6.3].

The Z score values in Table 2 show that the transcriptional networks are close to balanced (close-to-monotone) confirming observations in systems biology [59] that in such networks the number of edges whose removal eliminates negative cycles is small compared with the reshuffled networks. This explains the stability shown by such networks in response to external stimuli [59].

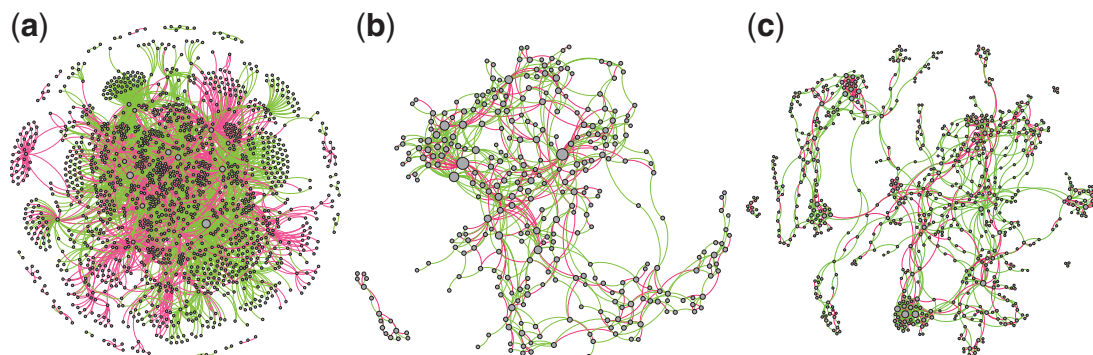


FIG. 3. Three biological signed networks visualized using Gephi. (a) The gene regulatory network of the *Escherichia coli* [61]. (b) Epidermal growth factor receptor pathway [62]. (c) Molecular interaction map of a macrophage [63].

TABLE 2 *The frustration index in biological networks*

Graph (n, m, m^-)	ρ	$L(G)$	$L(G_r) \pm SD$	Z score
Yeast (690, 1080, 220)	0.005	41	124.3 ± 4.97	-16.75
<i>Escherichia coli</i> (1461, 3215, 1336)	0.003	371	653.4 ± 7.71	-36.64
EGFR (329, 779, 264)	0.014	193	148.96 ± 5.33	8.26
Macrophage (678, 1425, 478)	0.006	332	255.65 ± 8.51	8.98

Removing the frustrated edges from yeast network, we obtain the monotone subsystem (induced subgraph) whose response to perturbations can be predicted from the underlying structure [35, 59]. Figure 4 shows the yeast network and its corresponding monotone subsystem obtained by removing the frustrated edges. In the monotone subsystem represented in Figure 4b all walks connecting two given nodes have one specific sign. This prevents oscillation and chaotic behaviour [35, 59] and allows system biologists to predict how perturbing node A impacts on node B based on the sign of walks connecting A to B. All walks connecting nodes of the same colour (different colours) have a positive (negative) sign, which leads to a monotone relationship between perturbation of one node and the impact on the other node. In contrast for the two signalling networks, the level of frustration is very high, i.e., there are far more frustrated edges compared to the corresponding reshuffled networks. Networks of the EGFR protein and that of the macrophage are different from transcriptional networks in nature and our results show that they are far from balanced. This result is consistent with the discussions of Iacono *et al.* that EGFR and macrophage networks cannot be classified as close-to-monotone [17, p. 233].

Besides differences in network categories, one can see a structural difference between the transcriptional networks and signalling networks in Figures 3–4. Figures 3a and 4a show many high-degree nodes having mostly positive or mostly negative edges in the two transcriptional networks. However, such structures are not particularly common in the two signalling networks as visualized in Figure 3b–3c.

The levels of balance in the two networks of yeast and *E. coli* were previously measured in [3] using the frustration index as well as measures based on triangles and eigenvalues [8–10]. For these two networks, the levels of balance measured using eigenvalues and the frustration index were reported to be consistent. However, it was observed that the overall structure is not well reflected in the triangles

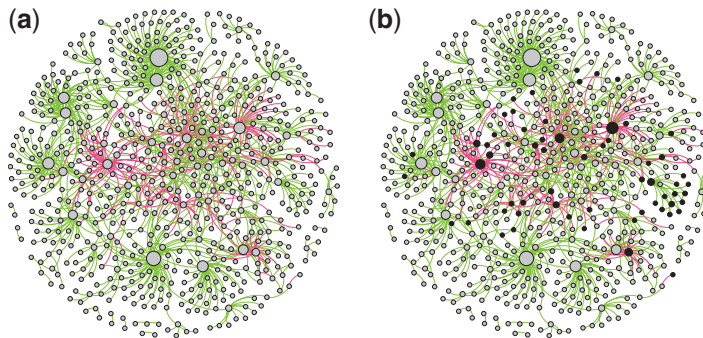


FIG. 4. The gene regulatory network of *Saccharomyces cerevisiae* [60] (a) and its monotone subsystem with optimal node colours (b) obtained after removing 41 frustrated edges.

because the small densities prevent the comparatively few triangles (70 triangles in yeast network and 1052 triangles in *E. coli* network) from representing the closeness of the two networks to balance [3].

6.3 Computations

The two smallest biological networks considered here (EGFR and macrophage) are the largest networks analysed in a recent study of balancing signed networks by negating minimal edges [48] in which the heuristic algorithm gives sub-optimal values of the frustration index [48, Fig. 5].

Aref *et al.* compare the quality and solve time of their exact algorithm with that of recent heuristics and approximations implemented on the same datasets [29, 30]. While data reduction schemes [27] may take up to 1 day for these four biological networks and heuristic algorithms [17] only provide bounds with up to 9% gap from optimality, the binary linear programming model (4) equipped with the speed-up techniques reaches global optimality in a few seconds on an ordinary computer [29, 30].

7. International relations

International relations between countries can be analysed using signed networks models and balance theory [64–66]. In earlier studies of balance theory, Harary used signed relations between countries over different times as an example of balance theory applications in this field [67].

7.1 Datasets

In this section, we analyse the frustration index in a temporal political network of international relations. Doreian and Mrvar have used the Correlates of War (CoW) datasets [50] to construct a signed network with 51 sliding time windows each having a length of 4 years [19]. Joint memberships in alliances, being in unions of states and sharing inter-governmental agreements are represented by positive edges. Being at war (or in conflict without military involvement) and having border disputes or sharp disagreements in ideology or policy are represented by negative edges [19].

A dynamic visualization of the network can be viewed on YouTube video sharing website [68]. This temporal network represents more than half a century of international relations among countries in the post Second World War era starting with 1946–1949 time window and ending with 1996–1999 time window [19]. One may refer to [19, Section 3.4] for a detailed explanation of using sliding time windows

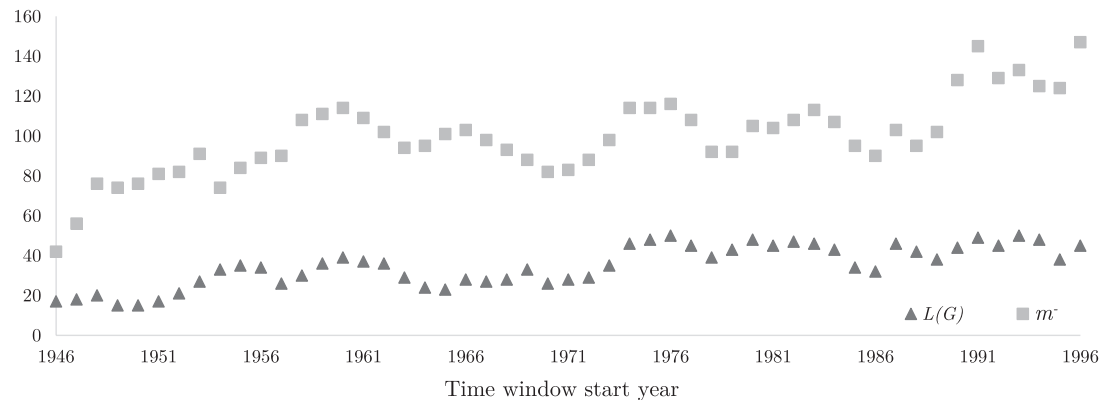


FIG. 5. The number of negative edges m^- and the frustration index $L(G)$ of the CoW dataset over time.

and other details involved in constructing the network. In the first time window of the temporal network, network parameters are $n = 64$, $m = 362$ and $m^- = 42$. In the last time window, these parameters are $n = 151$, $m = 1247$ and $m^- = 147$.

7.2 Results

Figure 5 demonstrates the number of negative edges and the frustration index in the CoW dataset. Doreian and Mrvar have attempted analysing the signed international network using the frustration index (under a different name) [19] and other measures. They used a blockmodeling algorithm in *Pajek* for obtaining the frustration index. However, their solutions are not optimal and thus do not give the frustration index for any of the 51 instances.

Even with reliable numerical results in hand, caution must be applied before answering whether this network has become closer to balance over the time period 1946–1999 [22, 69, 70] or the simpler question, how close this network is to total balance [3].

Using Z scores, we observe tens of standard deviation difference between the frustration index of 51 CoW instances and the average frustration index of the corresponding reshuffled graphs. This indicates that the network has been comparatively close to a state of structural balance over the 1946–1999 period. This is contrary to the evaluation of balance by Doreian and Mrvar using their frustration index estimates [19]. Bearing in mind that the size and order changes in each time window of the temporal network, we use the normalized frustration index, $F(G) = 1 - 2L(G)/m$, in order to investigate the partial balance over time. $F(G)$ provides values in the unit interval where the value 1 represents total balance. Figure 6 shows that all normalized frustration index values are greater than 0.86.

The data plotted in Figure 6 can also be used to statistically test the stationarity of the normalized frustration index values. The Priestley–Subba Rao (PSR) test of non-stationarity [71] provides the means of a statistically rigorous hypothesis testing for stationarity of time series. We use an R implementation of the PSR test that is available in the *fractal* package in the CRAN repository. The P -value of non-stationarity test for variation of $F(G)$ over time equals 0.03 indicating that there is strong evidence to reject the null hypothesis of stationarity.

While there is no monotone trend in the values of $F(G)$, in most years the network has moved towards becoming more balanced over the 1946–1999 period. The overlap of the time period with the Cold War

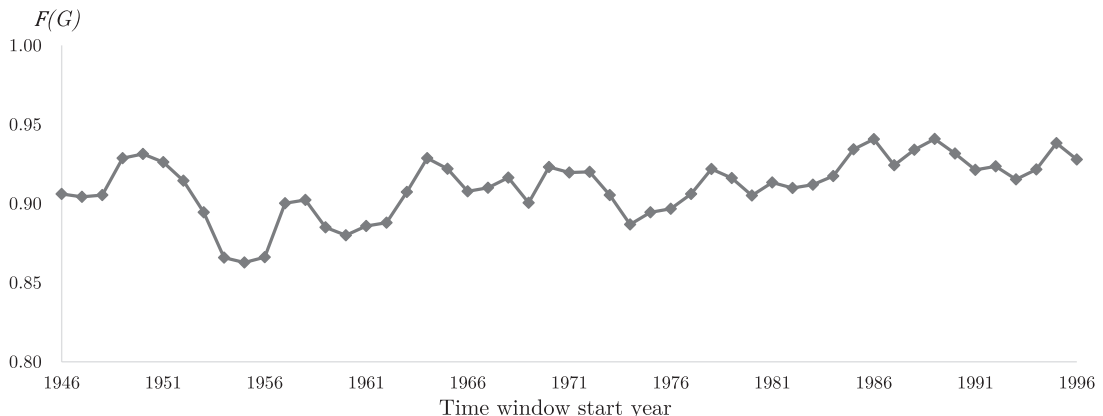


FIG. 6. The normalized frustration index in the CoW dataset over time.

era may explain how the network has been close to a global state of bi-polarity with countries clustered into two antagonist sides. Doreian and Mrvar claim to have decisive evidence [19] (based on frustration index estimates not showing monotonicity) against the theory [22, 69, 70] that signed networks evolve towards becoming more balanced. Our observations based on $F(G)$ values do not reject this theory.

7.3 Partitions

We can investigate how the 180 countries of the CoW dataset are partitioned into two internally solidary but mutually hostile groups in this network. The optimal node colours show that 32 countries have remained in one fixed partition, which we call group A, over 1946–1999 period. Group A includes Argentina, Belgium, Bolivia, Brazil, Canada, Chile, Colombia, Costa Rica, Denmark, Dominican Republic, Ecuador, El Salvador, France, Great Britain, Guatemala, Haiti, Honduras, Iceland, Italy, Luxembourg, Mexico, Netherlands, Nicaragua, Norway, Panama, Paraguay, Peru, Portugal, Turkey, Uruguay, United States and Venezuela. There are also 26 other countries that mostly (in over 40 time frames) belong to same partition as group A.

20 countries, which we call group B, oppose Group A in over 40 time frames. Group B includes North Korea, Sudan, Tunisia, Morocco, Libya, Kuwait, Algeria, German Democratic Republic (East Germany), Guinea, Syria, Egypt, Iraq, Jordan, Lebanon, Russia, Saudi Arabia, Cambodia, Mongolia, China and Yemen.

The remaining 102 countries change partition several times over 1946–1999 period. Figure 7 shows the partitioning of the countries in which Groups A and B are positioned on the right and left sides respectively. The countries that mostly belong to Group A partition are positioned at the bottom of Figure 7. The countries more inclined towards Group B are positioned closer to the top left side of Figure 7.

7.4 Computations

For this dataset, the binary linear programming model provides the exact values of the frustration index in less than 0.1 s on an ordinary computer with an Intel Core i5 7600 @ 3.50 GHz processor and 8.00 GB of RAM [29].

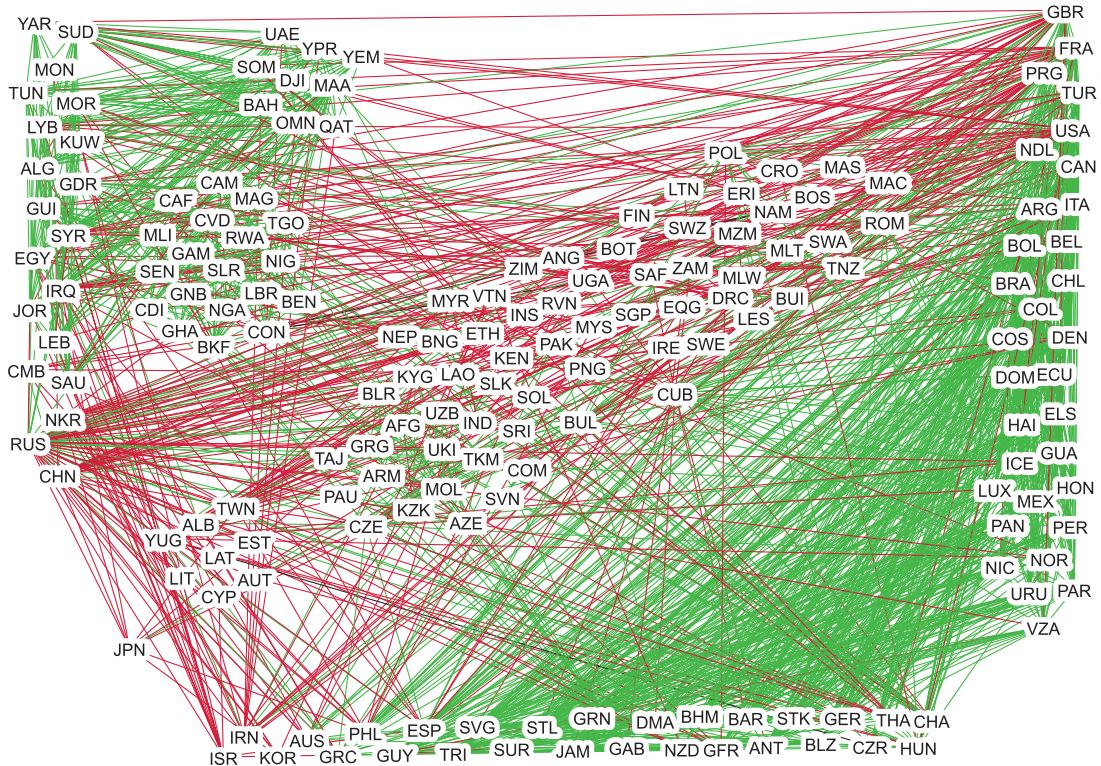


FIG. 7. The partitioning of countries into Groups A (right) and B (left) with most intra-group (inter-group) edges being positive (negative), the countries positioned in the bottom mostly belong to the same partition as Group A.

8. Financial portfolios

There are studies investigating financial networks of securities modelled by signed graphs [22, 27, 72]. Harary *et al.* originally suggested analysing portfolios using structural balance theory [22]. They represented securities of a portfolio by nodes and the correlations between pairs of securities by signed edges [22]. They used ± 0.2 as thresholds for considering a signed edge between two securities of a portfolio. Simplifying a portfolio containing Dow Jones, London FTSE, German DAX and Singapore STI to a signed graph with four nodes, they observed that the graph has remained in a state of balance from October 1995 to December 2000 [22]. Hüffner, Betzler and Niedermeier considered portfolios containing 60–480 stocks and thresholds of ± 0.325 , ± 0.35 , ± 0.375 to evaluate the scalability of their algorithm for approximating the frustration index [27]. Their dataset is also analysed in [72].

8.1 Datasets

In this subsection, we consider well-known portfolios recommended by financial experts for having a low risk in most market conditions [73]. These portfolios are known as lazy portfolios and usually contain a small number of *well-diversified* securities [73]. We consider six lazy portfolios each consisting of 5–11 securities. Table 3 represents the six lazy portfolios and their securities.

TABLE 3 *Six portfolios and their securities*

Portfolio	Ivy portfolio (P1)	Simple portfolio (P2)	Ultimate Buy & Hold (P3)	Yale Endow-ment (P4)	Swensen's lazy portfolio (P5)	Coffee House (P6)
Financial expert	Mebane Faber	Larry Swedroe	Paul Merriman	David Swensen	David Swensen	Bill Schultheis
VEIEX		x	x	x	x	
VGSIX			x	x	x	x
VIPSX		x	x	x	x	
VTMGX			x	x	x	
VIVAX		x	x			x
NAESX		x	x			x
EFV		x	x			
VFINX			x			x
VFISX			x		x	
VISVX			x			x
VTSMX				x	x	
IJS		x				
TLT				x		
VFITX			x			
VBMFX						x
VGTSX						x
GSG	x					
IEF	x					
VEU	x					
VNQ	x					
VTI	x					
<i>n</i>	5	6	11	6	6	7

The signed networks representing the lazy portfolios are generated by considering prespecified thresholds as in [22, 27]. We use the daily returns correlation data that can be found on the Portfolio Visualizer website [74] and thresholds of ± 0.2 similar to [22]. Correlation coefficients with an absolute value greater than 0.2 are considered to draw signed edges between the securities with respect to the sign of correlation. Figure 8 shows two networks of portfolio P3 based on the October 2016 data. The nodes represent 11 securities of the portfolio and the colours of the edges correspond to the correlations between the securities (green for positive and red for negative correlation). Lighter colours in Figure 8 (a) represent smaller absolute values of correlation coefficient.

8.2 Results

We analyse 108 monthly time frames for each of the six portfolios which correspond to the signed networks of each month within the 2008–2016 period. The signed networks obtained are totally balanced

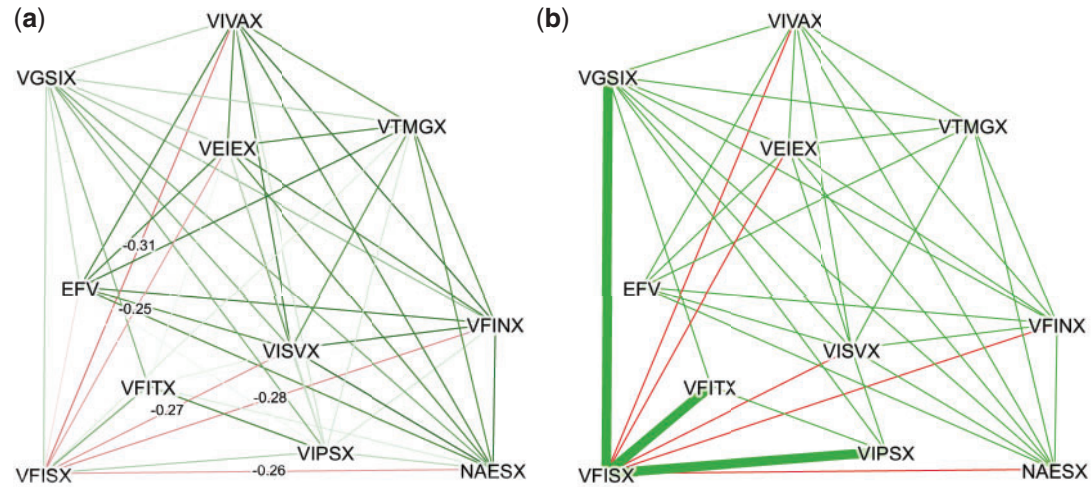


FIG. 8. Portfolio P3 in 2016–10 (unbalanced) illustrated as (a) weighted and (b) signed networks using Gephi. (a) A weighted complete graph representing correlation coefficients, edge weights ≤ -0.2 are shown on the edges. (b) The portfolio signed graph produced by thresholding on ± 0.2 , frustrated edges are shown by thick lines.

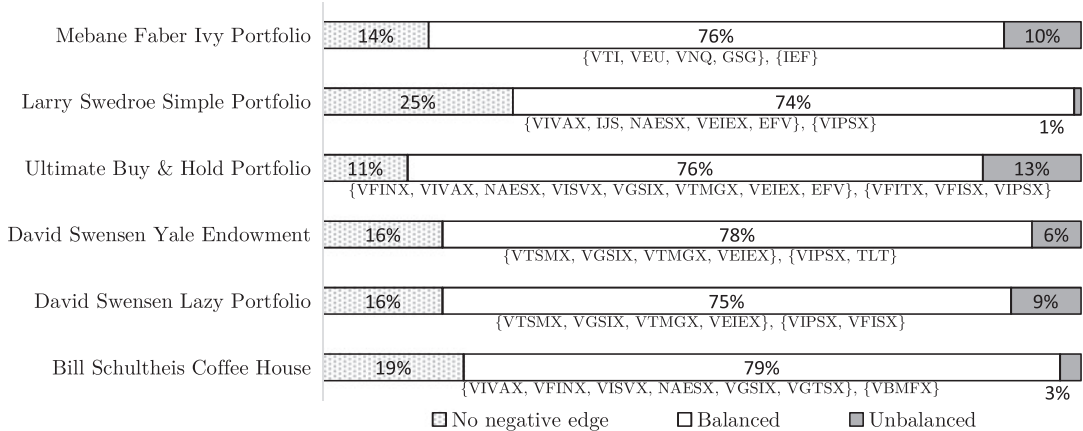


FIG. 9. Frequencies of all-positive, balanced, and unbalanced networks over 108 monthly time frames.

and have negative edges in a large number of time frames (74–79%). In a relatively small number of time frames (1–13%), the underlying network is unbalanced. Figure 9 illustrates the results, which are consistent with the findings of Harary *et al.* in [22] in terms of balanced states being dominant.

More detailed results on balance states and frustration index of six portfolios over time are provided in Figure 10. We observe that there are some months when several portfolios have an unbalanced underlying signed graph (non-zero frustration index values). One may suggest that common securities explain this observation, but P(1) does not have any security in common with other portfolios which suggests otherwise. It can be observed from Figure 10 that non-zero frustration index values are rather rare and usually very small.

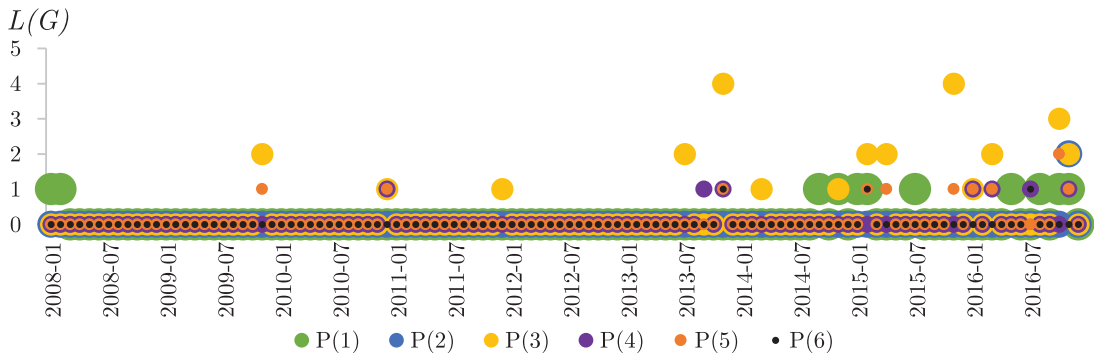


FIG. 10. Frustration index of six portfolios over 108 monthly time frames.

8.3 Partitions

The optimal partitioning of each portfolio into two sub-portfolios (with positive correlations within and negative correlations in between) can be obtained from optimal node colours. The optimal partitioning remains mostly unchanged over balanced states among 108 time frames. Figure 9 also shows the most common optimal partitioning of the securities for each portfolio.

8.4 Computations

Regarding sensitivity of the results to the cut-off threshold, other thresholds (like ± 0.1 and ± 0.3) also lead to balanced states being dominant. Using thresholds of ± 0.1 leads to relatively more unbalanced states and less all-positive states, while thresholds of ± 0.3 have the opposite effect. Regarding computational performance for these small instances, a basic optimization formulation of the problem with no speed-up technique (such as [30, Eq. 8]) would solve the portfolio instances in a reasonable time on an ordinary computer.

9. Closely related problems from chemistry and physics

In this section, we briefly discuss two problems from chemistry and physics that are closely related to the frustration index of signed graphs. The parallels between these problems and signed graphs allow us to use the binary linear model in (4) to tackle the NP-hard computation of important measures for relatively large instances. We discuss computation of a chemical stability indicator for carbon molecules in Subsection 9.1 and the optimal Hamiltonian of Ising models in Subsection 9.2.

9.1 Bipartivity of fullerene graphs

Previous studies by Došlić and associates suggest that graph bipartivity measures are potential indicators of chemical stability for carbon structures known as fullerenes [20, 23]. The graphs representing fullerene molecular structure are called fullerene graphs where nodes and edges correspond to atoms and bonds of a molecule, respectively. Došlić recommended the use of bipartivity measures in this context based on observing strong correlations between a bipartivity measure and several fullerene stability indicators. The correlations were evaluated on a set of eight experimentally verified fullerenes (produced in bulk quantities) with atom counts ranging between 60 and 84 [23]. Došlić suggested using the *spectral network*

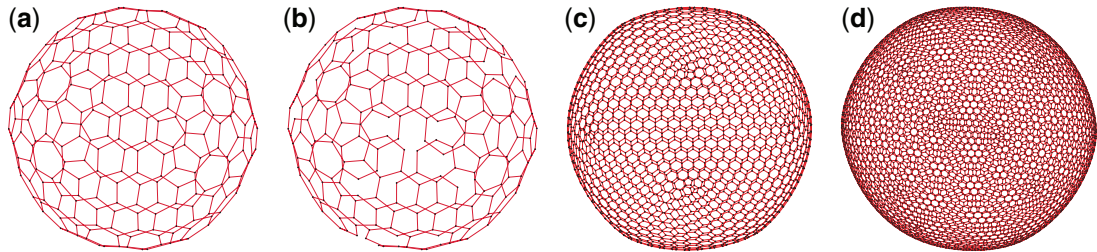


FIG. 11. Several fullerene graphs represented as signed graphs in which all edges are declared to be negative. (a) Fullerene graph of C240. (b) Fullerene graph of C240 made bipartite after removing 24 edges. (c) Fullerene graph of C2160. (d) Fullerene graph of C6000.

bipartivity measure, denoted by $\beta(G)$, which was originally proposed by Estrada *et al.* [75]. This measure equals the proportion of even-length to total closed walks as formulated in (5) in which λ_j ranges over eigenvalues of $|\mathbf{A}|$ (the entrywise absolute value of adjacency matrix \mathbf{A}). Note that $\beta(G)$ ranges between 0.5 and 1 and greater values represent more bipartivity.

$$\beta(G) = \frac{\sum_{j=1}^n \cosh \lambda_j}{\sum_{j=1}^n e^{\lambda_j}} \quad (5)$$

Two years later, Došlić and Vukičević suggested using the *bipartite edge frustration* as a more intuitive measure of bipartivity to investigate the stability of fullerenes [20]. This measure equals the minimum number of edges that must be removed to make the network bipartite [76, 77] and is closely related to the frustration index of signed graphs. Figure 11a shows a graph that is made bipartite in Figure 11b after removing 24 edges. Došlić and Vukičević have observed no strong correlation between the bipartite edge frustration and $\beta(G)$ [20]. However, both measures have performed well in detecting the most stable fullerenes among all isomers with 60 and 70 atoms [20]. More recently, Estrada *et al.* [78] proposed *spectral bipartivity index*, denoted as $b_s(G)$ and formulated in (6), as a bipartivity measure with computational advantages over $\beta(G)$. Note that $b_s(G)$ ranges between 0 and 1 and greater values represent more bipartivity.

$$b_s(G) = \frac{\sum_{j=1}^n e^{-\lambda_j}}{\sum_{j=1}^n e^{\lambda_j}} = \frac{\text{Tr}(e^{-\mathbf{A}})}{\text{Tr}(e^{\mathbf{A}})} \quad (6)$$

There are two other frustration-based measures of bipartivity suggested in [76]. Both measures are based on approximating $L(G)$ and we do not consider them.

9.1.1 Relevance The bipartite edge frustration of a graph is equal to the frustration index of the signed graph, G , obtained by declaring all edges of the fullerene graph to be negative. Using this analogy, we provide some results on the bipartivity of large fullerene graphs. According to Došlić *et al.*, a motivation for using the bipartite edge frustration is exploring the range of atom counts for which there are no confirmed stable isomers yet [20]. The least bipartite fullerene graphs represent the most stable fullerene isomers [20, 23]. Therefore, lower bipartivity (smaller values of $\beta(G)$, $b_s(G)$ and $F(G)$) can be interpreted as higher stability.

TABLE 4 Bipartivity measures computed for a range of large fullerene graphs

Fullerene graph	m	$L(G)$	$F(G)$	$\beta(G)$	$b_s(G)$
C180	270	18	0.86667	0.99765	0.99529
C240 [†]	360	24	0.86667	0.99823	0.99647
C260	390	24	0.87692	0.99837	0.99674
C320	480	24	0.9	0.99867	0.99735
C500	750	30	0.92	0.99915	0.99830
C540 [†]	810	36	0.91111	0.99921	0.99843
C720	1080	36	0.93333	0.99941	0.99882
C960 [†]	1440	48	0.93333	0.99956	0.99912
C1500 [†]	2250	60	0.94667	0.99972	0.99943
C2160 [†]	3240	72	0.95556	0.99980	0.99961
C2940 [†]	4410	84	0.96190	0.99986	0.99971
C3840 [†]	5760	96	0.96667	0.99989	0.99978
C4860 [†]	7290	108	0.97037	0.99991	0.99983
C6000 [†]	9000	120	0.97333	0.99993	0.99986

[†] Icosahedral fullerene.

9.1.2 Datasets We use the binary linear model in Eq. (4) to compute the bipartite edge frustration of several fullerene graphs with atom count ranging in 180 to 6000. The fullerene graph of C240 (molecule with 240 carbon atoms) and its bipartite subgraph are visualized in Figure 11a and 11b followed by C2160 and C6000 fullerene graphs in Figure 11c and 11d.

Among the 14 fullerene graphs we consider are the *icosahedral fullerenes* that have the structure of a truncated icosahedron. It is conjectured that this family of fullerenes has the highest chemical stability among all fullerenes with n atoms [20, 79].

9.1.3 Results The values of bipartivity measures for 14 fullerene graphs are computed in Table 4 where we have also provided the normalized frustration index, $F(G) = 1 - 2L(G)/m$, to compare the bipartivity of fullerenes with different atom counts. The closeness of $F(G)$, $\beta(G)$ and $b_s(G)$ values to 1 are consistent with fullerene graphs being almost bipartite (recall that these three measures take value 1 for a bipartite graph) [23].

Both spectral measures provide a monotone increase in the bipartivity values with respect to increase in atom count. However, $F(G)$ seems to provide distinctive values for icosahedral fullerenes. In particular for this set of fullerenes, we observe $F(C240) \neq F(C180)$, $F(C540) \neq F(C500)$ and $F(C960) \neq F(C720)$ which are consistent with the conjecture that icosahedral fullerenes are the most stable isomers [20, 79].

9.1.4 Computations Computing the bipartite edge frustration of a graph in general is computationally intractable and heuristic and approximation methods are often used instead [76]. For bipartite edge frustration of fullerene graphs which are planar; however, a polynomial time algorithm of complexity $O(n^3)$ exists [20]. Previous works suggest that this algorithm cannot process graphs as large as $n = 240$ [20]. Our computations for obtaining $L(G)$ of fullerene graphs with 180–2940 atoms take from split second to a few minutes. The solve times for computing $L(G)$ of C3840, C4860 and C6000 are 29.8, 68.1 and 97.5 min, respectively.

As indicated by Table 4 results, the optimization-based method in (4) allows computing frustration-based measures of bipartivity in the range of atom counts for which there are no experimentally verified stable isomers yet. The performance of frustration-based fullerene stability indicators requires further research that is beyond our discussion in this article.

9.2 Ising models with ± 1 interactions

Closely related to the frustration index of signed graphs, are the ground-state properties of Ising models. The most simple and standard form of Ising models represents patterns of atomic magnets based on interactions among spins and their nearest neighbours. A key objective in Ising models with ± 1 interactions is finding the spin configurations with the minimum energy [80]. The standard nearest-neighbour Ising model with ± 1 interactions and no external magnetic field is explained in what follows.

Each spin is connected to its neighbours in a grid-shaped structure. Two connected spins have either an aligned or an unaligned coupling. The positive (negative) interaction between two spins represents a coupling constant of $J_{ij} = +1$ ($J_{ij} = -1$) alternatively called matched (mismatched) coupling. Under another terminology from physics, positive and negative edges are referred to as ferromagnetic bonds and anti-ferromagnetic bonds respectively [81]. Each spin can either take an upward or a downward configuration. We discuss finding a spin configuration for a given set of fixed coupling constants that minimizes an energy function [80].

Frustration arises if and only if a matched (mismatched) coupling has different (same) spin configurations on the endpoints. The energy of a spin configuration is calculated based on the Hamiltonian function: $H = -\sum_{ij} J_{ij} s_i s_j$ in which the sum \sum_{ij} is over all the coupled spins. Note that J_{ij} represent the couplings limited to ± 1 in the Ising model with the type of interactions relevant to this study. Here s_1, s_2, \dots, s_n are the decision variables that take values $+1$ or -1 and represent upward/downward spin configurations. The Hamiltonian function of these Ising models is very similar to the energy function in [14] that is also used in other studies [17, 41, 46–48]. The problem of minimizing H over all possible spin configurations is NP-hard for many structures [82].

9.2.1 Relevance In order to make a connection between Ising models and signed graphs, we represent spins by nodes and spin configurations by node colours. Signs on the edges represent coupling constants where matched and mismatched couplings between spins are modelled as positive and negative edges, respectively.

If X^* represents the optimal colouring leading to $L(G)$ for a given signed graph, the minimum value of the corresponding Hamiltonian function can be calculated by $H(X^*) = -\sum_{ij} a_{ij}(2x_i - 1)(2x_j - 1)$. The minimum value of H is obtained based on the optimal spin configuration associated with X^* . Alternatively, one may consider the fact that frustrated edges and non-frustrated (satisfied) edges contribute values 1 and -1 to the Hamiltonian function, respectively. For an Ising model with m edges, this gives $H(X^*) = 2L(G) - m$ as the optimal Hamiltonian function value.

9.2.2 Datasets We use the binary linear model in Eq. (4) to compute the frustration index in Ising models of various grid size and dimension for several 2D and 3D grid structures as well as hypercubes. Figure 12 illustrates a 2D and a 3D Ising model with 50% unaligned couplings. Four hypercubes of dimension 4–7 with 50% unaligned couplings are visualized in Fig. 13.

For each Ising model, we generate 10 grids and randomly assign ± 1 to the edges to achieve the pre-defined proportion of negative edges based on our experiment settings. For each Ising model

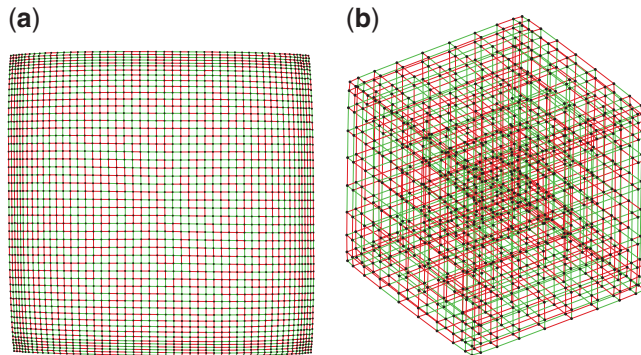


FIG. 12. Signed graphs with two and three dimensional structures representing simple Ising models with 50% unaligned couplings. (a) 2D Ising model 50×50 . (b) 3D Ising model $10 \times 10 \times 10$.

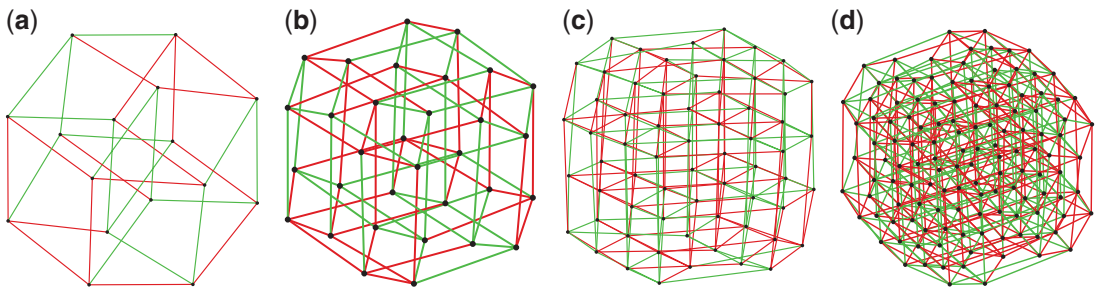


FIG. 13. Four signed graphs with hypercube structure representing more structurally complex Ising models with 50% unaligned couplings. (a) Dimension 4. (b) Dimension 5. (c) Dimension 6. (d) Dimension 7.

with a specific dimension and grid size, we consider three experiment settings with $m^-/m \in \{25\%, 50\%, 75\%\}$.

9.2.3 Results Table 5 provides results on Ising models with a fixed dimension and grid size in each row. The mean and standard deviation of the frustration index values and the average solve time (in seconds) for each experiment setting are provided in Table 5.

The results in Table 5 show that in most cases the Ising model with $m^-/m = 50\%$ has the highest frustration index value (and therefore, the highest optimal Hamiltonian value) among models with a fixed grid size and dimension. This can be explained by considering that in the structures investigated in Table 5 all cycles have an even length. Therefore a higher number of negative cycles (each containing at least one frustrated edge) is obtained when the number of positive and negative edges are equal.

9.2.4 Computations Hartmann *et al.* have suggested efficient algorithms for computing the ground-state properties in 3-dimensional Ising models with 1000 nodes [83] improving their previous contributions in 1-, 2- and 3-dimensional [21, 84, 85] Ising models. Recently, they have used a method for solving binary optimization models to compute the ground state of 3-dimensional Ising models containing up to 268^3 nodes [86]. While there are computational models for specialized Ising models based on the type

TABLE 5 *Frustration index values (and average solve times in seconds) for several Ising models*

Dimension, Grid size	$n,$ m	$m^-/m = 25\%$	$m^-/m = 50\%$	$m^-/m = 75\%$
		$L(G)$ mean \pm SD (solve time)	$L(G)$ mean \pm SD (solve time)	$L(G)$ mean \pm SD (solve time)
2, 50	2500, 4900	691.1 ± 12 (28.2)	720.9 ± 9.2 (31.9)	687.7 ± 10.5 (42.3)
2, 100	10 000, 19 800	2814.1 ± 16 (2452.3)	2938.2 ± 22.3 (2660.8)	2802.5 ± 24.7 (4685.2)
2, 150	22 500, 44 700	6416.1 ± 25.9 (5256.2)	6698.5 ± 55.3 (5002.0)	6396.3 ± 41.7 (6761.0)
2, 200	40 000, 79 600	11449 ± 47 (13140.6)	11930.3 ± 58.9 (12943.7)	11411.8 ± 46 (22720.4)
3, 5	125, 300	51.4 ± 1.7 (0.1)	52.4 ± 2.5 (0.1)	51 ± 3.2 (0.1)
3, 10	1000, 2700	491.5 ± 7.5 (82.9)	509.1 ± 4 (539.0)	491.6 ± 7 (96.4)
3, 15	3375, 9450	1762.1 ± 16.1 (8488.2)	1839.1 ± 10.4 (21384.3)	1761.1 ± 14.2 (9244.1)
4, 2	16, 32	5.6 ± 0.8 (0.1)	4.8 ± 1 (0.1)	5.6 ± 0.8 (0.1)
5, 2	32, 80	14.5 ± 1.1 (0.1)	15 ± 1.2 (0.1)	15 ± 1.2 (0.1)
6, 2	64, 192	38.8 ± 2 (0.1)	41 ± 1.6 (0.1)	38 ± 2.2 (0.1)
7, 2	128, 448	94.6 ± 3.1 (0.6)	99.6 ± 3.2 (1.6)	96 ± 2.4 (1.1)
8, 2	256, 1024	232.4 ± 3.7 (206.1)	245.8 ± 3.6 (4742.2)	231 ± 4.7 (543.87)

of underlying structure [21, 83–86], the binary linear programming model in Eq. (4) can be used as a general purpose computational method for finding the ground state of Ising models with ± 1 interactions regardless of the underlying structure.

10. Conclusion

In this study, the frustration index is used for analysing a wide range of signed networks from sociology and political science (Section 5), biology (Section 6), international relations (Section 7), finance (Section 8) and chemistry and physics (Section 9) unifying the applications of a fundamental graph-theoretic measure.

Our results contribute additional evidence that suggests many signed networks in sociology, biology, international relations and finance exhibit a relatively low level of frustration, which indicates that they are relatively close to the state of structural balance.

The numerical results also show the capabilities of the optimization-based model in Eq. 4 in making new computations possible for large-scale signed networks with up to 10^5 edges. The mismatch between exact optimization results we provided on social and biological networks in Sections 5–6 and those in the literature [14, 17, 27, 35, 41, 47] suggests the necessity of using accurate computational methods in analysing signed networks. This essential consideration is more evident from our results on international relations networks in Section 7 where inaccurate computational methods in the literature [19] have led to making a totally different inference with respect to the balance of signed international relations networks.

The current study provides extensive results on financial portfolio networks in Section 8 confirming the observations of Harary et al. [22] on small portfolio networks being mostly in a totally balanced state. In Section 9, we extended the applications of the frustration index to a fullerene stability indicator in Subsection 9.1 and the Hamiltonian of Ising models in Subsection 9.2. It is hoped that these discussions pave the way for using exact optimization models for more efficient and reliable computational analysis of signed networks, fullerene graphs and Ising models.

While this study provided an overview of the state-of-the-art of the numerical computations on signed graphs and the vast range of applications to which it can be applied, it is by no means an exhaustive survey on the applications of the frustration index. From a computational perspective, this and some other recent studies [87, 88] call for more advanced computational models that put larger networks within the reach of exact analysis. As another future research direction, one may consider formulating edge-based measures of stability for directed signed networks based on theories involving directionality and signed ties [13, 89].

Acknowledgements

The authors would like to show their gratitude to the Centre for eResearch at University of Auckland for providing the high performance computer and to Marco De La Pierre, Tomislav Došlić, and the anonymous referees for valuable comments and discussions that have improved this article.

REFERENCES

1. HEIDER, F. (1944) Social perception and phenomenal causality. *Psychol. Rev.*, **51**, 358–378.
2. CARTWRIGHT, D. & HARARY, F. (1956) Structural balance: a generalization of Heider's theory. *Psychol. Rev.*, **63**, 277–293.
3. AREF, S. & WILSON, M. C. (2018) Measuring partial balance in signed networks. *J. Complex Netw.*, doi: <http://doi.org/10.1093/comnet/cnx044> (last accessed 24 July 2018).
4. HARARY, F. (1957) Structural duality. *Behav. Sci.*, **2**, 255–265.
5. HARARY, F. (1959) On the measurement of structural balance. *Behav. Sci.*, **4**, 316–323.
6. NORMAN, R. Z. & ROBERTS, F. S. (1972) A derivation of a measure of relative balance for social structures and a characterization of extensive ratio systems. *J. Math. Psychol.*, **9**, 66–91.
7. HARARY, F. (1977) Graphing conflict in international relations. *Papers Peace Sci.*, **27**, 1–10.
8. TERZI, E. & WINKLER, M. (2011) A spectral algorithm for computing social balance. *Proceedings of International Workshop on Algorithms and Models for the Web-Graph, WAW 2011, Atlanta, Georgia, USA* (Frieze, A., Horn, P. & Prałat, P. eds). Berlin Heidelberg: Springer, pp. 1–13.
9. KUNEGIS, J. (2014) Applications of structural balance in signed social networks. *Physics*, arXiv: 1402.6865 (last accessed 24 July 2018).

10. KUNEGIS, J., SCHMIDT, S., LOMMATZSCH, A., LERNER, J., DE LUCA, E. W. & ALBAYRAK, S. (2010) Spectral analysis of signed graphs for clustering, prediction and visualization. *Proceedings of the 2010 SIAM International conference on Data Mining* (Parthasarathy, S., Liu, B., Goethals, B., Pei, J. & Kamath, C. eds), vol. 10. Philadelphia, PA, USA: Society for Industrial and Applied Mathematics, pp. 559–570.
11. PELINO, V. & MAIMONE, F. (2012) Towards a class of complex networks models for conflict dynamics. Preprint arXiv:1203.1394 (last accessed 24 July 2018).
12. ESTRADA, E. & BENZI, M. (2014) Walk-based measure of balance in signed networks: detecting lack of balance in social networks. *Phys. Rev. E*, **90**, 1–10.
13. LESKOVEC, J., HUTTENLOCHER, D. & KLEINBERG, J. M. (2010) Signed networks in social media. *Proceedings of the SIGCHI Conference on Human Factors in Computing Systems* (Mynatt, E. D., Schoner, D., Fitzpatrick, G., Hudson, S. E., Edwards, W. K. & Rodden, T. eds), CHI’10. New York, NY, USA: ACM, pp. 1361–1370.
14. FACCHETTI, G., IACONO, G. & ALTAFINI, C. (2011) Computing global structural balance in large-scale signed social networks. *Proc. Natl. Acad. Sci. USA*, **108**, 20953–20958.
15. ABELSON, R. P. & ROSENBERG, M. J. (1958) Symbolic psycho-logic: a model of attitudinal cognition. *Behav. Sci.*, **3**, 1–13.
16. ZASLAVSKY, T. (1987) Balanced decompositions of a signed graph. *J. Combin. Theor. Ser. B*, **43**, 1–13.
17. IACONO, G., RAMEZANI, F., SORANZO, N. & ALTAFINI, C. (2010) Determining the distance to monotonicity of a biological network: a graph-theoretical approach. *IET Syst. Biol.*, **4**, 223–235.
18. KASTELEYN, P. W. (1963) Dimer statistics and phase transitions. *J. Math. Phys.*, **4**, 287–293.
19. DOREIAN, P. & MRVAR, A. (2015) Structural balance and signed international relations. *J. Soc. Struct.*, **16**, 1–49.
20. DOŠLIĆ, T. & VUKIČEVIĆ, D. (2007) Computing the bipartite edge frustration of fullerene graphs. *Discrete Appl. Math.*, **155**, 1294–1301.
21. HARTMANN, A. K. (2011) Ground states of two-dimensional Ising spin glasses: fast algorithms, recent developments and a ferromagnet-spin glass mixture. *J. Stat. Phys.*, **144**, 519–540.
22. HARARY, F., LIM, M.-H. & WUNSCH, D. C. (2002) Signed graphs for portfolio analysis in risk management. *IMA J. Manag. Math.*, **13**, 201–210.
23. DOŠLIĆ, T. (2005) Bipartivity of fullerene graphs and fullerene stability. *Chem. Phys. Lett.*, **412**, 336–340.
24. SHERRINGTON, D. & KIRKPATRICK, S. (1975) Solvable model of a spin-glass. *Phys. Rev. Lett.*, **35**, 1792–1796.
25. BARAHONA, F. (1982) On the computational complexity of Ising spin glass models. *J. Phys. A Math. Gen.*, **15**, 3241–3253.
26. MÉZARD, M. & PARISI, G. (2001) The Bethe lattice spin glass revisited. *Eur. Phys. J. B*, **20**, 217–233.
27. F. HÜFFNER, BETZLER, N. & NIEDERMEIER, R. (2010) Separator-based data reduction for signed graph balancing. *J. Combin. Optim.*, **20**, 335–360.
28. KATAI, O. & IWAI, S. (1978) Studies on the balancing, the minimal balancing & the minimum balancing processes for social groups with planar and nonplanar graph structures. *J. Math. Psychol.*, **18**, 140–176.
29. AREF, S., MASON, A. J. & WILSON, M. C. (2017) An exact method for computing the frustration index in signed networks using binary programming. arXiv:1611.09030. url: <http://arxiv.org/pdf/1611.09030> (last accessed 24 July 2018).
30. AREF, S., MASON, A. J. & WILSON, M. C. (2018) Computing the line index of balance using integer programming optimisation. *Optimization Problems in Graph Theory* (Goldengorin, B. ed). Springer, 67–86. <https://www.springer.com/gp/book/9783319948294> (last accessed 24 July 2018).
31. FLAMENT, C. (1963) *Applications of Graph Theory to Group Structure*. Englewood Cliffs, NJ: Prentice-Hall.
32. HAMMER, P. L. (1977) Pseudo-boolean remarks on balanced graphs. *Numerische Methoden bei Optimierungsaufgaben Band 3: Optimierung bei graphentheoretischen und ganzzahligen Problemen* (Collatz, L., Meinardus, G. & Wetterling, W. eds), Basel, Switzerland: Birkhäuser, pp. 69–78.
33. BRAMSEN, J. (2002) Further algebraic results in the theory of balance. *J. Math. Sociol.*, **26**, 309–319.
34. BRUSCO, M. & STEINLEY, D. (2010) K-balance partitioning: An exact method with applications to generalized structural balance and other psychological contexts. *Psychol. Meth.*, **15**, 145–157.
35. DASGUPTA, B., G. ANDRES ENCISO, SONTAG, E. & ZHANG, Y. (2007) Algorithmic and complexity results for decompositions of biological networks into monotone subsystems. *Biosystems*, **90**, 161–178.

36. AGARWAL, A., CHARIKAR, M., MAKARYCHEV, K. & MAKARYCHEV, Y. (2005) $\mathcal{O}(\sqrt{\log n})$ approximation algorithms for min UnCut, min 2CNF deletion, and directed cut problems. *Proceedings of the Thirty-seventh Annual ACM Symposium on Theory of Computing* (Fagin, R. ed.), STOC'05, New York, NY, USA: ACM, pp. 573–581.
37. AVIDOR, A. & LANGBERG, M. (2007) The multi-multiway cut problem. *Theor. Comput. Sci.*, **377**, 35–42.
38. COLEMAN, T., SAUNDERSON, J. & WIRTH, A. (2008) A local-search 2-approximation for 2-correlation-clustering. *European Symposium on Algorithms* (Halperin, D. & Mehlhorn, K. eds), Karlsruhe, Germany: Springer, pp. 308–319.
39. DAVIS, J. A. (1967) Clustering and structural balance in graphs. *Hum. Relat.*, **20**, 181–187.
40. FIGUEIREDO, R. & MOURA, G. (2013) Mixed integer programming formulations for clustering problems related to structural balance. *Soc. Netw.*, **35**, 639–651.
41. MA, L., GONG, M., DU, H., SHEN, B. & JIAO, L. (2015) A memetic algorithm for computing and transforming structural balance in signed networks. *Knowl. Base. Syst.*, **85**, 196–209.
42. GIOTIS, I. & GURUSWAMI, V. (2006) Correlation clustering with a fixed number of clusters. *Proceedings of the Seventeenth Annual ACM-SIAM Symposium on Discrete Algorithm* (Stein, C. ed.), SODA'06, Philadelphia, PA, USA: Society for Industrial and Applied Mathematics, pp. 1167–1176.
43. DRUMMOND, L., FIGUEIREDO, R., FROTA, Y. & LEVORATO, M. (2013) Efficient solution of the correlation clustering problem: An application to structural balance. *On the Move to Meaningful Internet Systems: OTM 2013 Workshops* (Demey, Y. T. & Panetto, H. eds), Berlin, Heidelberg: Springer, pp. 674–683.
44. LEVORATO, M., DRUMMOND, L., FROTA, Y. & FIGUEIREDO, R. (2015) An ILS algorithm to evaluate structural balance in signed social networks. *Proceedings of the 30th Annual ACM Symposium on Applied Computing* (Bechini, A. & Hing, J. eds), SAC'15, Salamanca, Spain: ACM, pp. 1117–1122.
45. LEVORATO, M., FIGUEIREDO, R., FROTA, Y. & DRUMMOND, L. (2017) Evaluating balancing on social networks through the efficient solution of correlation clustering problems. *EURO J. Comput. Optim.*, **5**, 467–498.
46. ESMAILIAN, P., ABTAHI, S. E. & JALILI, M. (2014) Mesoscopic analysis of online social networks: the role of negative ties. *Phys. Rev. E*, **90**, 042817.
47. MA, L., GONG, M., YAN, J., YUAN, F. & DU, H. (2017) A decomposition-based multi-objective optimization for simultaneous balance computation and transformation in signed networks. *Inf. Sci.*, **378**, 144–160.
48. WANG, S., GONG, M., DU, H., MA, L., MIAO, Q. & DU, W. (2016) Optimizing dynamical changes of structural balance in signed network based on memetic algorithm. *Soc. Netw.*, **44**, 64–73.
49. FACCHETTI, G., IA CONO, G. & ALTAFINI, C. (2012) Exploring the low-energy landscape of large-scale signed social networks. *Phys. Rev. E*, **86**, 036116.
50. PEVEHOUSE, J., NORDSTROM, T. & WARNKE, K. (2004) The Correlates of War 2 international governmental organizations data version 2.0. *Conflict Manag. Peace Sci.*, **21**, 101–119.
51. GUROBI OPTIMIZATION INC. Gurobi optimizer reference manual, 2018. url: www.gurobi.com/documentation/8.0/refman/index.html (last accessed 1 March 2015).
52. HANSEN, P. (1978) Labelling algorithms for balance in signed graphs. *Problèmes Combinatoires et Théorie des Graphes* (Bermond, J. C., Fournier, J. C., Las Vergnas, M. & Sotteau, D. eds), Colloques Int. du CNRS, 260, Orsay, Paris, pp. 215–217.
53. HARARY, F. & KABELL, J. A. (1980) A simple algorithm to detect balance in signed graphs. *Math. Soc. Sci.*, **1**, 131–136.
54. AREF, S. (2017) Signed networks from sociology and political science, systems biology, international relations, finance, and computational chemistry. *Figshare Res. Data Repos.* doi: <http://doi.org/10.6084/m9.figshare.5700832.v2> (last accessed 24 July 2018).
55. READ, K. E. (1954) Cultures of the central highlands, New Guinea. *Southwest. J. Anthropol.*, **10**, 1–43.
56. SAMPSON, S. F. (1968) *A Novitiate in a Period of Change: An Experimental and Case Study of Social Relationships*. Ithaca, NY, USA: Cornell University.
57. NEAL, Z. (2014) The backbone of bipartite projections: Inferring relationships from co-authorship, co-sponsorship, co-attendance and other co-behaviors. *Soc. Netw.*, **39**, 84–97.
58. FOWLER, J. H. (2006) Legislative cosponsorship networks in the US House and Senate. *Soc. Netw.*, **28**, 454–465.

59. MA'AYAN, A., LIPSHTAT, A., IYENGAR, R. & SONTAG, E. D. (2008) Proximity of intracellular regulatory networks to monotone systems. *IET Syst. Biol.*, **2**, 103–112.
60. COSTANZO, M. C., CRAWFORD, M. E., HIRSCHMAN, J. E., KRANZ, J. E., OLSEN, P., ROBERTSON, L. S., SKRZYPEK, M. S., BRAUN, B. R., LENNON HOPKINS, K., KONDU, P., LENGIEZA, C., LEW-SMITH, J. E., TILLBERG, M. & GARRELS, J. I. (2001) YPDTM, PombePDTM and WormPDTM: model organism volumes of the BioKnowledgeTM Library, an integrated resource for protein information. *Nucleic Acids Res.*, **29**, 75–79.
61. SALGADO, H., GAMA-CASTRO, S., PERALTA-GIL, M., DIAZ-PEREDO, E., SÁNCHEZ-SOLANO, F., SANTOS-ZAVALET, A., MARTINEZ-FLORES, I., JIMÉNEZ-JACINTO, V., BONAVIDES-MARTINEZ, C., SEGURA-SALAZAR, J., MARTÍNEZ-ANTONIO, A. & COLLADO-VIDES, J. (2006) Regulondb (version 5.0): *Escherichia coli* k-12 transcriptional regulatory network, operon organization, and growth conditions. *Nucleic Acids Res.*, **34**, D394–D397.
62. ODA, K., MATSUOKA, Y., FUNAHASHI, A. & KITANO, H. (2005) A comprehensive pathway map of epidermal growth factor receptor signaling. *Mol. Syst. Biol.*, **1**.
63. ODA, K., KIMURA, T., MATSUOKA, Y., FUNAHASHI, A., MURAMATSU, M. & KITANO, H. (2004) Molecular interaction map of a macrophage. *AfCS Res. Rep.*, **2**, 1–12.
64. LAI, D. (2001) Alignment, Structural Balance & International Conflict in the Middle East, 1948–1978. *Conflict Manag. Peace Sci.*, **18**, 211–249.
65. DOREIAN, P., LLOYD, P. & MRVAR, A. (2013) Partitioning large signed two-mode networks: Problems and prospects. *Soc. Netw.*, **35**, 178–203.
66. LERNER, J. (2016) Structural balance in signed networks: separating the probability to interact from the tendency to fight. *Soc. Netw.*, **45**, 66–77.
67. HARARY, F. (1961) A structural analysis of the situation in the Middle East in 1956. *J. Conflict Resolut.*, **5**, 167–178.
68. AREF, S. (2017) Dynamic visualisation of the Correlates of War signed international relations network. YouTube video sharing website. <http://www.youtube.com/watch?v=STINsTjYjAQ> (last accessed 15 June 2017).
69. ANTAL, T., KRAPIVSKY, P. L. & REDNER, S. (2006) Social balance on networks: the dynamics of friendship and enmity. *Phys. D*, **224**, 130–136.
70. MARVEL, S. A., KLEINBERG, J. M., KLEINBERG, R. D. & STROGATZ, S. H. (2011) Continuous-time model of structural balance. *Proc. Natl. Acad. Sci. USA*, **108**, 1771–1776.
71. PRIESTLEY, M. B. & SUBBA RAO, T. (1969) A test for non-stationarity of time-series. *J. R. Stat. Soc. Ser B*, **31**, 140–149.
72. FIGUEIREDO, R. & FROTA, Y. (2014) The maximum balanced subgraph of a signed graph: Applications and solution approaches. *Eur. J. Oper. Res.*, **236**, 473–487.
73. BOGLE, J. C. (2015) *Bogle on Mutual Funds: New Perspectives for the Intelligent Investor*. Hoboken, NJ, USA: John Wiley & Sons.
74. Silicon Cloud Technologies. Portfolio visualizer asset correlations for lazy portfolios, 2017. url: <http://www.portfoliovisualizer.com/asset-correlations> (last accessed 3 July 2017).
75. ESTRADA, E. & RODRÍGUEZ-VELÁZQUEZ, J. A. (2005) Spectral measures of bipartivity in complex networks. *Phys. Rev. E*, **72**, 046105.
76. HOLME, P., LILJEROS, F., EDLING, C. R. & JUN KIM, B. (2003) Network bipartivity. *Phys. Rev. E*, **68**, 056107.
77. YANNAKAKIS, M. (1981) Edge-deletion problems. *SIAM Journal on Computing*, **10**, 297–309.
78. ESTRADA, E. & GÓMEZ-GARDEÑES, J. (2016) Network bipartivity and the transportation efficiency of european passenger airlines. *Phys. D*, **323–324**, 57–63.
79. FARIA, L., KLEIN, S. & STEHLIK, M. (2012) Odd cycle transversals and independent sets in fullerene graphs. *SIAM J. Discrete Math.*, **26**, 1458–1469.
80. FRIEDLI, S. & VELENIK, Y. (2017) *Statistical Mechanics of Lattice Systems: A Concrete Mathematical Introduction*. Cambridge, UK: Cambridge University Press.
81. ZASLAVSKY, T. (2018) Negative (and positive) circles in signed graphs: a problem collection. *AKCE International J. Graphs and Combinatorics*, **15**, 31–48.

82. LIERS, F., JÜNGER, M., REINELT, G. & RINALDI, G. (2004) *Computing exact ground states of hard Ising spin glass problems by branch-and-cut*. In: Hartmann, A. K. & Rieger, H. (eds), New optimization algorithms in physics. Berlin, Germany: Wiley-Blackwell, pp. 47–69.
83. MANSSEN, M. & HARTMANN, A. K. (2015) Matrix-power energy-landscape transformation for finding NP-hard spin-glass ground states. *J. Global Optim.*, **61**, 183–192.
84. DEWENTER, T. & HARTMANN, A. K. (2014) Exact ground states of one-dimensional long-range random-field Ising magnets. *Phys. Rev. B*, **90**, 014207.
85. MELCHERT, O. & HARTMANN, A. K. (2013) Information-theoretic approach to ground-state phase transitions for two-and three-dimensional frustrated spin systems. *Phys. Rev. E*, **87**, 022107.
86. FYTAS, N. G., THEODORAKIS, P. E. & HARTMANN, A. K. (2016) Revisiting the scaling of the specific heat of the three-dimensional random-field Ising model. *Eur. Phys. J. B*, **89**, 200.
87. GISCARD, P.-L., KRIEGE, N. & WILSON, R. C. (2016) A general purpose algorithm for counting simple cycles and simple paths of any length. Preprint arXiv:1612.05531 (last accessed 24 July 2018).
88. GISCARD, P.-L., ROCHE, P. & WILSON, R. C. (2017) Evaluating balance on social networks from their simple cycles. *J. Complex Netw.*, **5**, 750–775.
89. YAP, J. & HARRIGAN, N. (2015) Why does everybody hate me? Balance, status, and homophily: The triumvirate of signed tie formation. *Soc. Netw.*, **40**, 103–122.